Temperature-dependent reflectivity, dispersion parameters, and optical constants for $PbWO_4$

J. M. Stencel,* E. Silberman, and J. Springer
Fisk University, Nashville, Tennessee 37203

E. A. Jones
Vanderbilt University, Nashville, Tennessee 37235

(Received 28 May 1976)

Polarized infrared reflectivity measurements of $PbWO_4$ were made from 45 to 4000 cm^{-1} at 300°K, and from 220 to 4000 cm^{-1} at 100°K. Raman spectra were also obtained at 300°K. The infrared spectra were analyzed using classical-oscillator and Kramers-Kronig dispersion theories. The temperature-dependent changes in the oscillator strengths and the damping constants, along with frequency shifts, are discussed. Near-infrared and visible reflectivity measurements are reported which clarify discrepancies between experimental reflectivities at 4000 cm^{-1} and those calculated using visible dielectric constants. Two-phonon modes in the LO-TO regions of the $PbWO_4$ ν_3 band are shown to explain its complex nature, while providing reasons for apparent discrepancies in reflectivity fits for other scheelites.

I. INTRODUCTION

Large single crystals of lead tungstate, and others with scheelite structure, can be easily grown by the Czochralski method. These crystals have intense absorption bands which make high-quality transmission spectra difficult to obtain unless ultrathin samples are used. However, they provide an excellent opportunity for obtaining good bulk-reflectivity spectra. The vibrational spectra of $CaWO_4$ and $CaMoO_4$ were first successfully characterized by reflection techniques,[1] but very little was discussed about the reststrahlen band fine structure due to two-phonon modes. In the present work, we report eight infrared-allowed fundamental mode frequencies of $PbWO_4$ including three formerly unknown frequencies. The complex ν_3 band contour is shown to be the result of at least four combination bands, which were assigned from infrared and Raman data obtained from the same oriented sample. The comparison of the dispersion analysis results at 300 °K with those at 100 °K, along with the polarized reflectivity of the ν_3 band at 50 °K, are used in clarifying the temperature-dependent spectral changes.

II. EXPERIMENTAL

The large single $PbWO_4$ crystal obtained for this study was ellipsoidal in shape, with major and minor axes of approximately 3 and 2 cm. It was oriented by back-reflection x-ray Laue photography, cut with a diamond saw, and polished so its $\vec{a}$-$\vec{c}$ axes were within $\pm \frac{1}{2}^\circ$ of the resultant faces. Small pits could be distinguished on the sample surface when viewed under a microscope, but these had no effect on the shape or intensity of the infrared reflection bands to within experimental error.

Polarized reflection spectra were taken for the electric field E parallel and perpendicular to the sample $\vec{c}$ axis. A Beckman IR-11 (33–800 cm^{-1}), Beckman IR-12 (200–4000 cm^{-1}), and Cary 14 (4000–50 000 cm^{-1}) spectrometer were used for data acquisition. A Spectra-Physics 4-W argon-ion laser and a Beckman 700 spectrometer were used for obtaining the Raman spectra. A specially built reflection mirror system, sample chamber, and positioning table enabled dry-air purging for the total optical path of the infrared instruments.[2] Each infrared spectrum was encoded and recorded on paper tape, with data sampling taken at intervals between 0.1 and 0.5 cm^{-1}. Then, each was standardized by comparing it to a freshly aluminized mirror, assumed to have an absolute reflectivity as given by Ehrenreich *et al.*,[3] and averaged with two other standardized spectra. All measure-

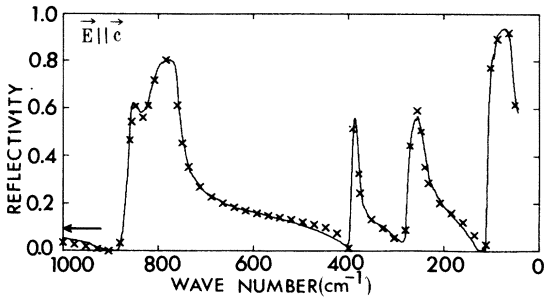

FIG. 1. Reflectivity of $PbWO_4$ at 300 °K for the electric vector E parallel to the $\vec{c}$ axis. The X's show the best fit obtained with the classical oscillator dispersion equation. In this and succeeding figures the arrow shows the reflectivity at 4000 cm^{-1}; from 1600 to 4000 cm^{-1} the reflectivity is approximately this constant value.

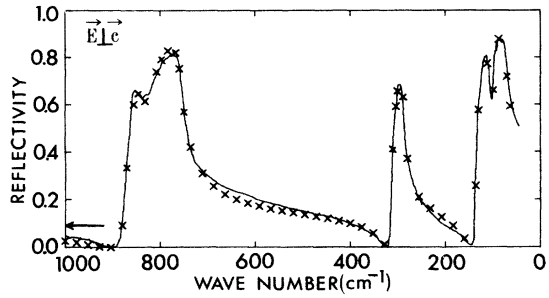

FIG. 2. Reflectivity of $PbWO_4$ at 300 °K for the electric vector E perpendicular to the $\vec{c}$ axis. The X's show the best fit obtained with the classical oscillator dispersion equation.

ments were obtained with an angle of incidence of about 8°. Figures 1 and 2 show the resultant room-temperature spectra, while Figs. 3 and 4 show those obtained at 100 °K. The spectral reproducibility is 1% from 600 to 4000 cm^{-1}, and 3% from 45 to 600 cm^{-1}. The curve with the X's are the result of the fits using the dispersion theory, which will be described below.

III. ANALYSIS

Group-theoretical analysis of the scheelite structures C_{4h}^6 space group gives the distribution of the vibrations into the irreducible representations as

$$\Gamma = 3A_g + 5B_g + 5E_g + 4A_u + 3B_u + 4E_u ,$$

where A_g, B_g, and E_g are Raman active, while A_u and E_u and E_u are infrared active. The Raman spectra of $PbWO_4$ and the assignment of its bands has been given by Khana *et al.*[4] Table I shows the Raman frequencies we have obtained; we find no B_g-E_g splitting at 350 cm^{-1}, while the internal mode frequencies are larger than the published values.

Classical dispersion (CD) theory applied to the

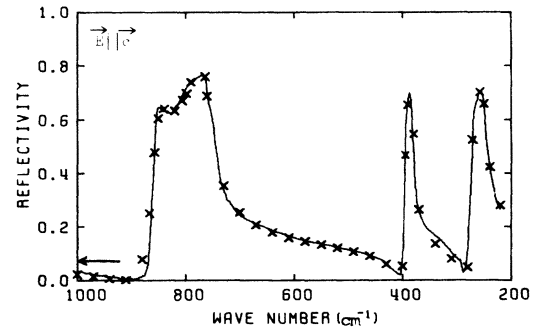

FIG. 3. Reflectivity of $PbWO_4$ at 100 °K for the electric vector E parallel to the $\vec{c}$ axis. The X's show the best fit obtained with the classical oscillator dispersion equation.

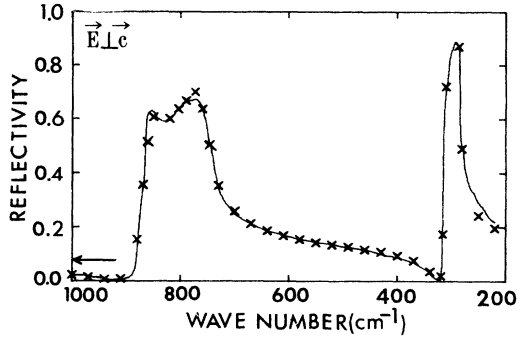

FIG. 4. Reflectivity of $PbWO_4$ at 100 °K for the electric vector E perpendicular to the $\vec{c}$ axis. The X's show the best fit obtained with the classical oscillator dispersion equation.

determination of the complex dielectric constant $\epsilon(\nu)$ of a material leads to

$$\epsilon(\nu) = \epsilon_\infty + \sum_{j=1}^{n} \frac{S_j \nu_j^2}{\nu_j^2 - \nu^2 + i\gamma_j \nu} ,$$

where ϵ_∞ is the high-frequency dielectric constant which neglects the molecular vibrational contributions, and ν_j, S_j, and γ_j are the mode frequencies, oscillator strengths, and damping constants, respectively. The sum is intended to cover the n oscillators needed to reproduce the reflectivity spectrum. Kramers-Kronig inversion of the reflectivity R has also been used to obtain the optical constants $\epsilon_1(\nu)$ and $\epsilon_2(\nu)$, where $\epsilon(\nu) = \epsilon_1(\nu) + i\epsilon_2(\nu)$. This method should give exact values for ϵ_1 and ϵ_2, independent of any model. However, it has not been widely used because it may yield physically impossible negative absorption coefficients near the reststrahlen bands due to the difficulty of obtaining accurate data over a wide enough spectral range. Recent application of high-energy extrapolation procedures,[5] evaluation of systematic errors in the measurement of reflectivities R,[6] and the use of superconvergence and sum rules[7] have provided means of constraining the Kramers-Kronig results to physically possible situations.

TABLE I. Raman frequencies and assignments for $PbWO_4$ at 300 °K.

A_g (cm^{-1})	B_g (cm^{-1})	E_g (cm^{-1})	Assignment
905			ν_1 (W-O Stretch)
	766	753	ν_3 (W-O bend)
	358	358	ν_4 (WO_4^{--} bend)
328	328		ν_2 (WO_4^{--} bend)
		192	Rotation (xy)
178			Rotation (z)
	54	63	Pb^{++}-Pb^{++} translation
	78	90	WO_4^{--}-WO_4^{--} translation

Our Kramers-Kronig analysis covering an interval of integration from 0 to 33 000 cm^{-1}, in conjunction with a systematic error analysis for regions of low reflectivity, shows that the measurement error should be kept below 1% over the entire data region in order to enable the correction procedure in complex spectra to be satisfactory. This is a result of having the error in the R measured at any frequency ν causing distortion in the optical constants at all frequencies. Our room-temperature CD results, shown in Table II, yielded the eight infrared-allowed frequencies whose mode assignments agree with Tarte *et al.*[8] We have been able to separate the two ν_3 fundamental modes (A_u, E_u), and have obtained the frequency of the previously unknown A_u translational mode (58 cm^{-1}). Although the CD analysis is in reality a conjecture, it has been shown to agree with quantum-mechanical results near resonant frequencies,[9] and has been highly successful even for complex spectra which require a large number of poles.[10]

Reflection spectra can be valuable in determining accurate fundamental frequencies. This is seen in the 4-cm^{-1} spread in the frequencies reported for the intense ν_3 band for $NaNO_3$ (approximately 135 cm^{-1}),[11,12] as compared with the 65-cm^{-1} spread obtained from transmission spectra.[13,14] This example shows the necessity of having very-thin crystals, sometimes less than 5 μm thick, for accurate frequency determinations using transmission spectroscopy. The only method of assigning a frequency to a strong absorption band is to assume it occurs at the transmission minimum, or in the middle of the absorption region. But, absorption peaks for relatively thick crystals occur at the corresponding reflection maximum, not necessarily at the mode frequency. Use of thick crystals for transmission work had led to incorrect frequency assignments in the past,[15] while the neglect of possible reflection effects has also caused false spectral interpretations.[16] The fundamental infrared frequency values for crystalline $PbWO_4$, as shown in Tables II and III, are thus believed to be more accurate than previously reported values, even taking into account the relative importance of the γ/ν ratio,[17] and the method used in the pole fit.[18]

Each CD pole fit was obtained from initial approximate dispersion parameters, followed by a minimization routine which calculated covariance matrix elements to minimize the function

$$\sum_{i=1}^{n}\left(\frac{(R_i - R_{\mathrm{CD}\,i})^2}{n} - 1\right)^{1/2},$$

where $R_{\mathrm{CD}\,i}$ is the calculated reflectivity, and R_i is the experimental reflectivity at each data point i. Differences between the experimental spectra

TABLE II. Classical oscillator dispersion (CD) parameters for $PbWO_4$ at 300 °K. ν_l are longitudinal frequencies; ν_m are multiphonon frequencies whose assignments are given in Table V.

	ν_j (cm^{-1})	S_j (cm^{-2})	γ_j (cm^{-1})	ν_l (cm^{-1})	
		$\vec{E}\perp\vec{c}$			
R [a]	73	12.9	5.9	101	
T [b]	104	0.50	10.1	137	
ν_4	288	0.81	8.2	314	
ν_3	756	1.04	12.1	869	
ν_m	801	0.014	18.0		
ν_m	821	0.009	19.7	$\epsilon_\infty = 3.63$ [c]	
ν_m	825	0.005	17.1	$\epsilon_0 = \epsilon_\infty + \sum_{j=1}^{n} S_j = 18.92$ [d]	
ν_m	837	0.007	17.3		
		$\vec{E}\parallel\vec{c}$			
T	58	15.73	3.68	109	
ν_4	251	1.05	11.7	278	
ν_2	384	0.22	4.31	393	
ν_3	764	0.851	9.11	866	
ν_m	786	0.024	15.4		
ν_m	804	0.015	16.4	$\epsilon_\infty = 3.67$	
ν_m	821	0.013	17.8	$\epsilon_0 = 21.55$	
ν_m	834	0.013	19.5		

[a] R is the rotation; [b] T^+ is the translation.

[b] T is the translation.

[c] The indices of refraction in the visible region as given in the *Handbook of Chemistry and Physics* (Chemical Rubber Co., Cleveland, 1968) would predict: ϵ_∞ ($\vec{E}\parallel\vec{c}$) = 5.19 and ϵ_∞ ($\vec{E}\perp\vec{c}$) = 4.79.

[d] Reference 20 has ϵ_0 ($\vec{E}\parallel\vec{c}$) = 31.0 and ϵ_0 ($\vec{E}\perp\vec{c}$) = 23.6.

TABLE III. CD parameters for $PbWO_4$ at 100 °K. ν_l are longitudinal frequencies; ν_m are multiphonon frequencies.

	ν_j (cm^{-1})	S_j (cm^{-2})	γ_j (cm^{-1})	ν_l (cm^{-1})	
		$\vec{E}\perp\vec{c}$			
ν_4	285	0.97	2.86	313	
ν_3	758	0.891	19.3	873	
ν_m	789	0.025	19.2		
ν_m	802	0.016	19.0		
ν_m	812	0.010	15.4	$\epsilon_\infty = 3.17$	
ν_m	820	0.005	17.1		
ν_m	825	0.005			
ν_m	836	0.006			
		$\vec{E}\parallel\vec{c}$			
ν_4	248	1.26	8.17	275	
ν_2	381	0.354	4.58	397	
ν_3	757	0.889	15.2	869	
ν_m	784	0.019	18.9		
ν_m	801	0.012	19.4		
ν_m	813	0.008	18.4	$\epsilon_\infty = 3.27$	
ν_m	821	0.003	18.2		
ν_m	823	0.005	18.3		
ν_m	835	0.002	13.7		

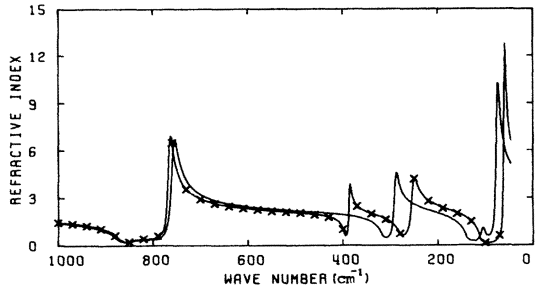

FIG. 5. Refractive indices of $PbWO_4$ at 300 °K for the electric vector E parallel to the $\vec{c}$ axis (XX) and perpendicular to the $\vec{c}$ axis (solid line).

and the dispersion fit are evident at approximately 650, 320, and 220 cm^{-1}. These regions are associated with poor spectrometer response due to low reflectivity and residual atmospheric absorption, but could also have contributions from combination bands. Differences seen for the complex ν_3 region (ca. 800 cm^{-1}) attest to the difficulty encountered in obtaining a reasonable fit here. Tables II and III give the dispersion parameters used for these fits, along with the longitudinal frequencies ν_l, and the dielectric constants. We note that at least five oscillators were necessary to fit the complex ν_3 band and that the dielectric constants are considerably lower than those predicted from visible data. Figures 5–8 show the refractive indices and extinction coefficients for $PbWO_4$ at the two experimental temperatures, as we calculated them with the CD theory.

The $CaWO_4$ pole fit (see Barker, Ref. 1) shows modes which are forbidden by $k \simeq 0$ selection rules. High-reflectivity regions are characterized by negative ϵ_1, being very sensitive to ϵ_2 even where it is much smaller than ϵ_1. Small changes in ϵ_2 thus produce significant fine structure only in regions of relatively high reflectivity. Table IV shows the reported "forbidden" mode frequencies, along with two-phonon mode frequencies calculated from the infrared and Raman spectra.[1,4]

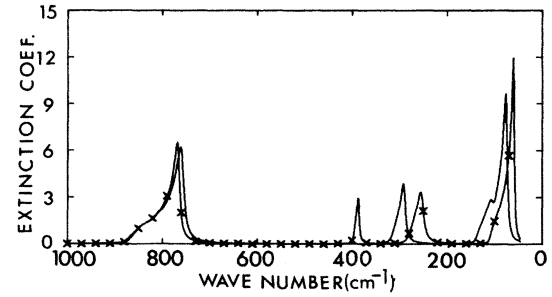

FIG. 6. Extinction coefficients of $PbWO_4$ at 300 °K for the electric vector E parallel to the $\vec{c}$ axis (XX) and perpendicular to the $\vec{c}$ axis (solid line).

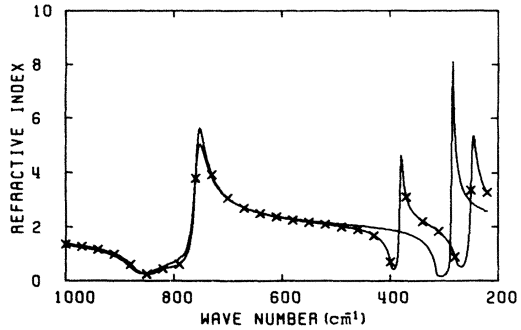

FIG. 7. Refractive indices of $PbWO_4$ at 100 °K for the electric vector E parallel to the $\vec{c}$ axis (XX) and perpendicular to the $\vec{c}$ axis (solid line).

The apparent discrepancies seen for the $CaWO_4$ pole fit can then be attributed to contributions to the molecular polarization from two-phonon modes. Similarly, the ν_3 band of $PbWO_4$ shows structure which is expected to be a result of two-phonon modes; 20 possible two-phonon modes could lie in the LO-TO region of this band. Large dipole-dipole interactions could be an extremely important intermode mixing mechanism, as indicated by the large LO-TO splitting of the ν_3 band. Also, two-phonon modes may not originate from the center of the Brillouin zone, producing modes which appear in both polarizations. Table V shows the two-phonon assignments for this region. The calculated frequencies ν_c were obtained from the polarized Raman and infrared spectra of the same oriented crystal.

Besides this fine structure, the calculated high-frequency ϵ_∞ dielectric constants of both $PbWO_4$ and $CaWO_4$ are considerably below the measured visible dielectric constants. Our spectra had an approximate 6% reflectivity increase over the near-infrared region (4000–12 000 cm^{-1}), with relatively constant reflectivity in the visible (12 000–25 000 cm^{-1}), thus accounting for the dielectric constant difference. The near-infrared

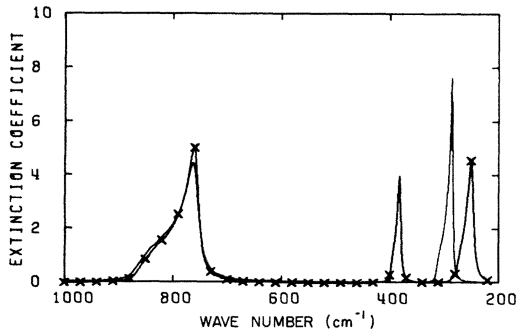

FIG. 8. Extinction coefficients of $PbWO_4$ at 100 °K for the electric vector E parallel to the $\vec{c}$ axis (XX) and perpendicular to the $\vec{c}$ axis (solid line).

TABLE IV. "Forbidden" mode frequencies of $CaWO_4$ (ν_f), and two-phonon mode frequencies ν_c calculated from the infrared and Raman spectra (Ref. 1 and 4).

$\vec{E} \perp \vec{c}$		$\vec{E} \parallel \vec{c}$	
ν_c (cm^{-1})	ν_f (cm^{-1})	ν_c (cm^{-1})	ν_f (cm^{-1})
319, 353, 354, 360	322	259, 260, 266, 324	275
223, 239	213		
838	840		
893	894		

dispersion can be attributed to an absorption wing of the electronic bands near 3000 Å.[19] This also explains partially the calculated static dielectric constant ϵ_0 being 27% below the measured values,[20] but even a pole-fit attempt using the visible dielectric constants gave ϵ_0 values which were 10% too small. This indicates significant contributions to ϵ_0 from unseen combination bands and/or electronic absorption bands.

A. Damping constants

The quantum-mechanical interpretation of the damping constant γ is that it results primarily from phonons that are coupled together through cubic terms in the Hamiltonian. When evaluated at ν_j, Maradudin and Wallis's treatment of γ_j/ν_j takes the form[21]

$$\gamma_j(\nu, T)/\nu_j = (\text{const}/\nu_j^4)\,[(e^{h\nu_j/kT} - 1)^{-1} + \tfrac{1}{2}] .$$

As the temperature decreases the ratio γ_j/ν_j should become smaller reaching a minimum at 0 °K, which is not zero, but is described by the zero-point energy of the oscillator. This shows that cubic anharmonic potential terms grow smaller at $T \to 0$ °K, and that molecular vibrations at lower temperatures can be described to a better approximation by harmonic oscillations. Correspondingly, reflectivities should approach unity. Table VI lists γ/ν values for the fundamental modes for which temperature-dependent effects could be studied in this experiment. Only two of five ratios decrease, suggesting these two modes have cubic potential terms dominating their behavior. The anomalous behavior of the others can be investigated by a close inspection of the ν_3 reflection band obtained at 50 °K, as shown in Fig. 9.

We note that the reflectivity of the main resonance continues to decrease, while the summation region remains relatively constant. The intensity dependence of the summation region is

$$1 + n_j + n_k + n_j n_k ,$$

where n_j and n_k are the occupation numbers of the fundamental ν_j and ν_k modes.[22] As the temperature is decreased, ν_j and ν_k become more harmonic, while n_j and n_k decrease, resulting in the reduction of the integrated intensity of the summation band. In spite of this reduction, the peak intensity may increase or stay constant because of the decrease in the damping constant γ. The combination of these two processes could cause a constant reflectivity; the 836-, 835-, and 820-cm^{-1} bands have lower S_j and γ_j for the 100 °K spectra. This implies that they result from cubic- or higher-order anharmonic potential terms. The other two-phonon modes could be the result of large dipole-dipole interactions, whose intensities are quadratically dependent on the phonon coordinates. Their larger γ_j and relatively constant S_j reduce their contributions to the fine structure, while allowing the band at 820 cm^{-1} to be more pronounced. The fact that the ν_3 bands also decrease in reflectivity as the temperature is lowered cannot be explained in terms of cubic anharmonicity,

TABLE V. Multiphonon-mode assignments for $PbWO_4$. ν_c are frequencies calculated from the Raman frequencies and the fundamentals of the infrared spectra, and ν_m are frequencies obtained from the CD analysis.

300 °K		100 °K		
ν_m (cm^{-1})	ν_c (cm^{-1})	ν_m (cm^{-1})	ν_c (cm^{-1})	Assignment
786	789	784, 789	789	$2\nu_4 + R(E_u)$
801	801	801	801	$\nu_3(E_g) + T(A_u)$
804	803	802	803	$\nu_1(A_g) - T(E_u)$
		812, 813	812	$\nu_3(E_u) + T(B_g)$
825	827	820	820	$\nu_3(A_u) + T(E_g)$
821	819	821	821	$\nu_3(E_u) + T(E_g)$
		823, 825	826	$\nu_3(E_g) + R(E_u)$
834	834	835	836	$\nu_3(E_u) + T(B_g)$
837	839	836	839	$\nu_3(B_g) + R(E_u)$

TABLE VI. γ_j/ν_j ratios for the fundamentals of $PbWO_4$.

γ_j/ν_j (300 °K)	γ_j/ν_j (100 °K)	Mode
0.028	0.010	$\nu_4(E_u)$
0.047	0.033	$\nu_4(A_u)$
0.011	0.012	$\nu_2(A_u)$
0.012	0.020	$\nu_3(A_u)$
0.016	0.025	$\nu_3(E_u)$

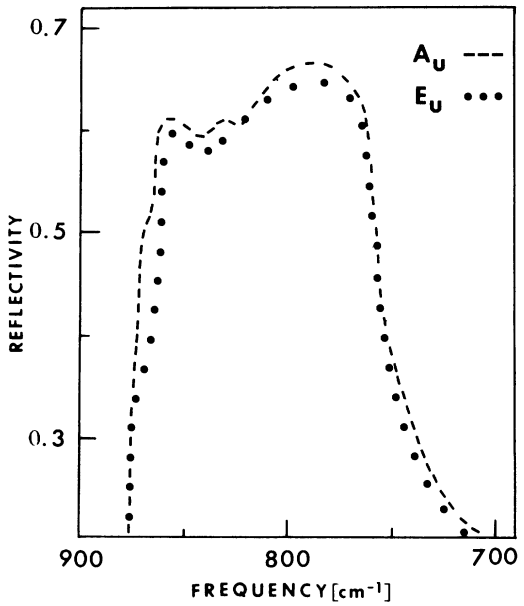

FIG. 9. Reflectivity of the ν_3 band of $PbWO_4$ at 50 °K for the electric vector E parallel to $\vec{c}$ axis (dashed line) and perpendicular to the $\vec{c}$ axis (dotted line).

but may have its origin in large dipole-dipole interactions.

B. Frequency shifts

The temperature-dependent frequency shifts $\Delta\nu = \nu_{300\,^\circ K} - \nu_{100\,^\circ K}$ of the $\nu_4(A)$ and $\nu_4(E)$ modes can be expressed in terms of volume-dependent shifts $\Delta\nu_v$ and anharmonicity shifts $\Delta\nu_\gamma$:

$$\Delta\nu_E = \Delta\nu_{Ev} + \Delta\nu_{E\gamma} , \tag{1}$$

$$\Delta\nu_A = \Delta\nu_{Av} + \Delta\nu_{A\gamma} . \tag{2}$$

Comparison of Tables II and III shows γ for $\nu_4(E)$ decreases by 5.34 while γ for $\nu_4(A)$ decreases only 3.53. The larger damping constant change for the $\nu_4(E)$ mode should cause a larger anharmonicity-dependent frequency shift. At the two experimental temperatures we can thus write

$$\Delta\nu_{A\gamma} \simeq c\Delta\nu_{E\gamma} ,$$

where c is a constant and $c < 1$. Substituting into Eqs. (1) and (2), along with the fact that $\Delta\nu_E = \Delta\nu_A = -3$ cm^{-1}, gives the following general relations:

$$\Delta\nu_\gamma < 0 \text{ when } \Delta\nu_{Ev} > \Delta\nu_{Av} , \tag{3}$$

$$\Delta\nu_\gamma > 0 \text{ when } \Delta\nu_{Av} > \Delta\nu_{Ev} . \tag{4}$$

Equation (4) implies that both $\Delta\nu_v$ for ν_4 can only be negative. Negative $\Delta\nu_v$'s are not impossibilities, but all $\Delta\nu_v$ for the alkali halides are positive. Equation (3) which leads to $\Delta\nu_v > 0$ is therefore more likely to be true. If so, it shows that the contribution of the cubic anharmonicity to the $\Delta\nu_4$'s is negative when lowering the temperature from 300 to 100 °K. It also indicates larger volume-dependent shifts for the $\nu_4(E_u)$ mode than for $\nu_4(A_u)$. The frequency shifts of the ν_3 modes might also indicate similar behavior, but the anomalous temperature dependence of their reflectivities, and the interactions with the lattice modes, complicates possible interpretations.

IV. CONCLUSIONS

We have obtained the frequencies of the individual ν_3 modes and the previously unknown translation A_u frequency through the interpretation of the polarized infrared reflection spectra of $PbWO_4$. The contributions of two-phonon modes to regions of high reflectivity have been shown to be significant for modes of large LO-TO splitting. High-frequency dielectric constants needed to reproduce accurately the reflectivity spectra were shown to be considerably smaller than those suggested from visible data, which resulted from dispersion of the optical constants in the near infrared. The analysis of spectra obtained at different temperatures showed the cubic anharmonicity dominates the behavior of the ν_4 fundamentals, but was unable to explain the temperature dependence of ν_3. Also when comparing the two polarizations of ν_4, the assumption of larger damping constant changes is related with larger anharmonicity-dependent frequency shifts has allowed the comparision of the volume-dependent shifts of the ν_4 modes, while showing that the anharmonicity shifts are negative in the 300–100 °K temperature range.

ACKNOWLEDGMENTS

It is a pleasure to acknowledge the cooperation of W. S. Brower (Inorganic Materials Division, National Bureau of Standards) for supplying the $PbWO_4$ crystal and of O. B. Cavin (Metals and Ceramics Div., Oak Ridge National Laboratories) for the crystal orientation. It is also a pleasure to acknowledge the invaluable help of H. W. Morgan and P. Staats (Oak Ridge National Laboratories).

*Work done in partial fulfillment of Ph.D. requirements at Vanderbilt University.

[1]A. S. Barker, Jr., Phys. Rev. 135, A742 (1964).
[2]Ph.D. dissertation, J. M. Stencel, Vanderbilt University (1976) (unpublished).
[3]H. Ehrenreich, H. R. Philipp, and B. Segall, Phys. Rev. 132, 1918 (1963).
[4]R. K. Khana, W. S. Brower, B. R. Guscott, and E. R. Lippincott, J. Res. Natl. Bur. Stand. (U. S.) A 72, 81 (1968).
[5]R. S. Bauer, W. E. Spicer, and J. J. White, III, J. Opt. Soc. Am. 64, 830 (1974).
[6]Che-Kuang Wu and G. Anderman, J. Opt. Soc. Am. 58, 519 (1968).
[7]H. W. Ellis and J. R. Stevenson, J. Appl. Phys. 46, 3066 (1975).
[8]P. Tarte and M. Liegeouis-Duyckaerts, Spectrochim. Acta A 28, 2029 (1972).
[9]J. R. Jasperse, A. Kahan, J. N. Plendl, and S. S. Mitra, Phys. Rev. 146, 526 (1966).
[10]W. G. Spitzer and D. A. Kleinman, Phys. Rev. 121, 1324 (1961).
[11]K. H. Hellewege, W. Lesch, M. Plihal, and G. Schaack, Z. Phys. 232, 61 (1970).
[12]J. A. Ketelaar, C. Haas, and J. Fahrenfort, Physica 20, 1259 (1954).
[13]R. Eckhardt, D. Eggers, and L. J. Slutsky, Spectrochim. Acta A 26, 2033 (1970).
[14]H. G. Hafele, Z. Phys. 148, 262 (1957).
[15]R. K. Khana and E. R. Lippincott, Spectrochim. Acta A 24, 905 (1968).
[16]F. Bessette and A. Cabana, Spectrochim. Acta A 25, 157 (1969).
[17]A. S. Barker, Jr., Phys. Rev. 136, A1290 (1964).
[18]A. Kachare, G. Anderman, and L. R. Brantley, J. Phys. Chem. Solids, 33, 467 (1972).
[19]W. van Loo, Phys. Status Solidi 27, 565 (1975).
[20]W. S. Brower, Jr., and P. H. Fang, J. Appl. Phys. 40, 4988 (1969).
[21]A. A. Maradudin and R. F. Wallis, Phys. Rev. 125, 4 (1962).
[22]C. H. Perry and N. E. Tornberg, Phys. Rev. 183, 595 (1969).